Ocean Dynamics (2016) 66:605–621
DOI 10.1007/s10236-016-0936-0

Subsurface hydrographic structures and the temporal variations of Aleutian eddies

Rui Saito[1] · **Ichiro Yasuda**[1] · **Kosei Komatsu**[1,2] · **Hiromu Ishiyama**[3] · **Hiromichi Ueno**[4] · **Hiroji Onishi**[4] · **Takeshi Setou**[5] · **Manabu Shimizu**[5]

Received: 29 June 2015 / Accepted: 17 February 2016 / Published online: 17 March 2016

Abstract Aleutian eddies are mesoscale anticyclonic eddies formed within the Alaskan Stream region between 180° meridian and 170° E south of the Aleutian Islands. They propagate southwestward after the isolation from the Alaskan Stream and pass through the Western Subarctic Gyre. We compared hydrographic structures of three Aleutian eddies observed during summer, west of 170° E (Eddy A) and east of 170° E (Eddies B and C). In each eddy, a subsurface dichothermal water (3.0–4.0 °C) was observed above a subsurface mesothermal water (4.0–4.5 °C). The minimum temperature in the dichothermal water at around a depth of 100 m was colder in Eddy A (2.8 °C) than in Eddies B and C (3.0–3.2 °C). This difference could be ascribed to wintertime cooling and influence of surrounding waters during spring warming period. The wintertime cooling makes the dichothermal water colder for eddies isolated from the Alaskan Stream region for a longer time. Particle-tracking experiments using re-analysis products from a data-assimilative eddy resolving ocean model suggested that the dichothermal water within Eddy A was cooled by the entrainment of surrounding colder water even during the spring warming period. The mesothermal waters at depth around 250 m demonstrated similarity among the observed eddies, and the maximum temperature in the mesothermal water within Eddy A (4.3 °C) was close to that of Eddies B and C (4.2 °C) in the in situ observations. These results indicated that the dichothermal water of Aleutian eddies modifies over time, whereas the mesothermal water maintains the original feature as they propagate southwestward from the Alaskan Stream region to the Western Subarctic Gyre.

Keywords Aleutian eddy · Hydrographic structure · Aleutian Islands · Alaskan stream

Responsible Editor: Pierre De Mey

Electronic supplementary material The online version of this article (doi:10.1007/s10236-016-0936-0) contains supplementary material, which is available to authorized users.

✉ Rui Saito
rsaito@aori.u-tokyo.ac.jp

[1] Atmosphere and Ocean Research Institute, The University of Tokyo, 5-1-5 Kashiwanoha, Kashiwa, Chiba 277-8564, Japan

[2] Graduate School of Frontier Sciences, The University of Tokyo, 5-1-5 Kashiwanoha, Kashiwa, Chiba 277-8564, Japan

[3] Graduate School of Environmental Science, Hokkaido University, 3-1-1 Minato-cho, Hakodate, Hokkaido 041-8611, Japan

[4] Faculty of Fisheries Sciences, Hokkaido University, 3-1-1 Minato-cho, Hakodate, Hokkaido 041-8611, Japan

[5] Fisheries Research Agency, National Research Institute of Fisheries Science, 2-12-4 Fukuura, Kanazawa, Yokohama, Kanagawa 236-8648, Japan

1 Introduction

The Alaskan Stream is the northern boundary current in the subarctic Pacific (Favorite 1967; Ohtani 1973; Ohtani et al. 1997; Reed and Stabeno 1999). This current primarily flows westward along the south of Alaska Peninsula and the Aleutian Islands from the head of the Gulf of Alaska (about 145° W) to the Near Strait (about 172° E) (Fig. 1a). Several branches of the current pass through passes and straits of the archipelago and enter the Bering Sea (Reed and Stabeno 1993). The Alaskan Stream functions as a connection between the Alaska Gyre and the Bering Sea Gyre or the Western Subarctic Gyre (Onishi and Ohtani 1999; Onishi 2001) (Fig. 1a).

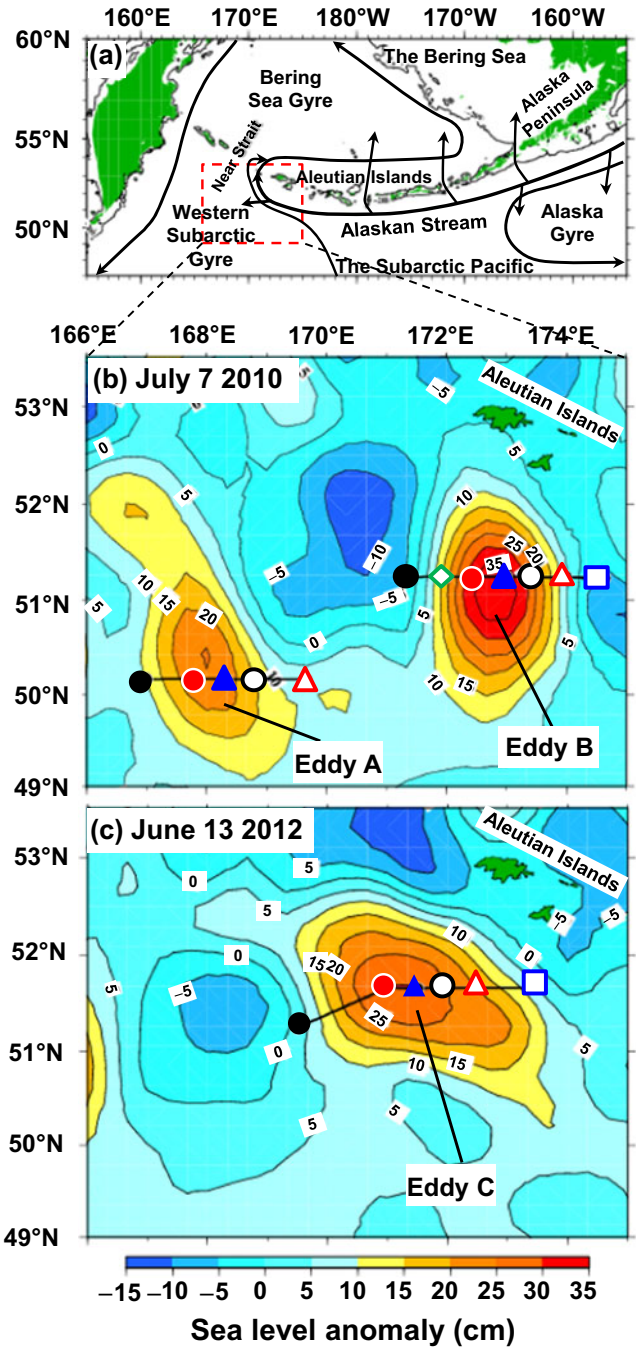

Fig. 1 **a** The geographical location of present study area south of Aleutian Islands in the subarctic Pacific. General circulations, the Alaska Gyre (AG), the Bering Sea Gyre (BSG), and the Western Subarctic Gyre (WSG) are also shown (referred to Ohtani 1973). **b** Locations of observing stations along lines crossing mesoscale anticyclonic eddies (Aleutian eddies) on July 7, 2010, and **c** a line crossing an Aleutian eddy on June 13, 2012, superimposed by AVISO sea level anomaly (*color contour*). The same symbols are used in Figs. 1, 2, and 3 for each eddy

Anticyclonic eddies along the Alaskan Stream and the coast of the Gulf of Alaska transport significant mass of coastal water together with heat, freshwater, macro- and micronutrients, phytoplankton, and zooplankton to the offshore open ocean (Crawford 2005; Crawford et al. 2007; Brown et al. 2012; Ikenoue et al. 2012; Ueno et al. 2012). These eddies play key roles in offshore biological production. Along the Alaskan Stream between 157 and 169° W, Alaskan Stream eddies are known to be formed (Ueno et al. 2009). These eddies propagate westward for 1 to 5 years, often traverse the 180° meridian, and enter the Western Subarctic Gyre.

The other type of mesoscale anticyclonic eddies appear in the western Alaskan Stream region between 180° meridian and the south of Near Strait (about 170° E) and are called "Aleutian eddies." Many of Aleutian eddies propagate southwestward and reach as far as about 160° E in the Western Subarctic Gyre (Rogachev et al. 2007; Rogachev and Shlyk 2009). A recent study (Prants et al. 2013) using a Lagrangian surface flow model computed from AVISO surface velocity field demonstrated that mesoscale eddies including Aleutian eddies controlled the surface flow direction and flux through the Near Strait. The model study clarified that eddies possibly affected surface flow south of Aleutian Islands and through the strait. However, eddy activities below the surface, especially in the subsurface layers remain uncertain.

In the subarctic Pacific, north of 40° N, dichothermal water (subsurface temperature minimum) and mesothermal water (subsurface temperature maximum, underneath the minimum) are ubiquitous features related with the strong permanent halocline (Ueno and Yasuda 2000, 2005; Ueno et al. 2005; 2007). In winter, surface mixed layer becomes the coldest in vertical profile because stratification in the subarctic North Pacific is maintained by increasing salinity with depth. The dichothermal water is thus formed by winter surface cooling and subsequent surface warming during spring and summer when the base of winter mixed layer remains as a temperature minimum. In the western subarctic Pacific, including the formation and propagation regions of Aleutian eddies, dichothermal water outcrops during winter and is often preserved throughout the year (Ueno et al. 2005). In the eastern subarctic Pacific, temperature minimum sometimes outcrops in winter, and dichothermal water vanishes in autumn. Hydrographic vertical sections of Aleutian eddies including subsurface structures have been demonstrated by only two eddies. Rogachev et al. (2007) firstly reported a section of an Aleutian eddy propagating northwestward near 165° E, where subsurface dichothermal water (subsurface temperature minimum) with 2.4–3.4 °C at a depth of 50–200 m and subsurface mesothermal water (subsurface temperature maximum) of 3.4–3.8 °C at 200–500 m depth were observed. The other section was observed in an Aleutian eddy south of the Aleutian Islands near 173° E, within the Alaskan Stream region, where dichothermal water of 3.0–3.5 °C at a depth of 70–200 m and mesothermal water of 3.0–4.5 °C at 200–500 m depth were observed (Saito et al. 2014). The temperature of

subsurface dichothermal water was different between the two eddies. Saito et al. (2014) also found greater abundance and lipid accumulation of zooplankton (large calanoid copepods) within the colder subsurface dichothermal water in the Aleutian eddy than that warmer outside. Subsurface dichothermal water could have potential impact on lower trophic level ecosystems; however, the hydrographic structures and temporal changes of Aleutian eddies have not been fully understood due to insufficient in situ observations and analyses.

In the present study, we synthesize in situ observations and model analysis of Aleutians eddies to clarify the hydrographic structures and temporal variations. In the summers of 2010 and 2012, we observed three different Aleutian eddies, two of them observed west of 170° E and an eddy observed east of 170° E on board T/S Oshoro-maru, School of Fisheries Sciences, Hokkaido University, Japan. We firstly compared hydrographic structures of these three Aleutian eddies and described the difference in the dichothermal water. Then, we evaluated the history of eddies especially by describing temporal changes in the dichothermal water using a re-analysis dataset generated by an eddy resolving ocean model. Based on the results of particle-tracking experiments, using velocity estimates from the re-analysis dataset, we proposed possible causes of the difference in the subsurface dichothermal water within the observed eddies.

2 Data and methods

2.1 In situ data

In situ observations were conducted at five stations along 50° 10′ N from 167° 00′ to 169° 39′ E at seven stations along 50° 40′ N from 176° 24′ to 178° 44′ E on July 7, 2010 (Fig. 1b). On June 13, 2012, in situ data were collected at one station at 51° 15′ N, 169° 30′ E and five stations along 51° 39′ N from 169° 29′ to 173° 29′ E (Fig. 1c). We performed the observations on board T/S Oshoro-maru (School of Fisheries Sciences, Hokkaido University, Japan). At each station, temperature and salinity were measured using a conductivity-temperature-depth profiler (CTD) (Sea Bird Electronics, Inc., USA, CTD-SBE 9plus) or an expendable CTD (XCTD) (Tsurumi Seiki Co., Ltd., Japan, XCTD-2). The physical oceanographic data in 2010 were published in Hokkaido University (2011).

2.2 Satellite data

Based on the delayed-time maps of sea level anomalies (SLA) of a merged-altimeter satellite data, distributed at 7-day intervals from Archiving, Validation, and Interpretation Satellite Oceanographic (AVISO), with support from Collecte Localisation Satellites (2014), SSALTO/DUACS, France (http://www.aviso.oceanobs.com/duacs), each transect crossed a mesoscale anticyclonic eddy with SLA of 10–35 cm and diameter of about 200–400 km in the present study area. We named a western eddy in 2010 in which a 50° 40′ N transect crossed as "Eddy A," an eastern eddy where a 50° 40′ N transect crossed as "Eddy B," and an eddy in 2012 as "Eddy C." Eddy B which we previously analyzed in Saito et al. (2014) was re-examined to compare with other observed Aleutian eddies and to explain difference in the subsurface dichothermal waters. To evaluate position of mesoscale anticyclonic eddies, we examined the delayed time data of SLA with the spatial resolution of 1/4° × 1/4° at 7-day intervals from October 14, 2009 to June 13, 2012. During summer, water expands as water temperature increases; therefore, the use of raw SLA data results in the whole region to be positive during summer and negative during winter (Ueno et al. 2012). For that reason, the weekly spatial mean SLA of the subarctic Pacific north of 45° N except the marginal seas was subtracted from each weekly map of SLA to compensate for seasonal steric effect (Ueno et al. 2009, 2010, 2012). We tracked eddies by Okubo-Weiss parameter (Okubo 1970; Weiss 1991) calculated from SLA (h) assuming geostrophy. Velocities were calculated from SLA using the following equations. Zonal (U) and meridional (V) velocities were computed as

$$U = -\frac{g}{f}\frac{\partial h}{\partial y}, V = \frac{g}{f}\frac{\partial h}{\partial x}$$

where g is gravity, f is Coriolis parameter, and h is SLA. Okubo-Weiss parameter (W) was evaluated as

$$W = S_n^2 + S_s^2 - \omega^2$$

where S_n ($=U_x - V_y$) and S_s ($=V_x + U_y$) are normal and shear components of strain, respectively, and ω ($=V_x - V_y$) is vorticity. U and V are zonal and meridional components of velocity, respectively, and x and y are orthogonal spatial coordinates. Following Chelton et al. (2007), we defined an area with $W < -2 \times 10^{-12}$ s^{-2} as an eddy area. Eddy area and location of eddy center were estimated. Individual eddies were tracked in the same approach as Henson and Thomas (2008), Inatsu (2009), and Ueno et al. (2012). The location of eddy center may have errors >50 km due to the data resolution and eddy propagation (Ladd et al. 2005, 2007). To determine when an Aleutian eddy was isolated from the Alaskan Stream region, we used 1/4° × 1/4° grid delayed time data of absolute dynamic topography (ADT), which demonstrates the flow area of the Alaskan Stream at 7-day intervals from October 14, 2009 to June 13, 2012 from AVISO with support from Collecte Localisation Satellites (2014).

Sea surface temperature was obtained from Physical Oceanography Distributed Active Archive Center

(PODAAC), National Aeronautics and Space Administration (NASA), USA, as the Group of High Resolution Sea Surface Temperature Science Team (GHRSST) (2011) during winter and spring to check consistency between temperature change in a re-analysis data and the observed value.

2.3 Climatological dataset

1° × 1° grid climatological net surface heat flux (NOC1.1 Flux Climatology, National Oceanographic Centre, UK, http://noc.ac.uk) (Grist and Josey 2003) from sea surface to atmosphere (heat flux in upward direction) was used to estimate temperature changes in the approximate areas of observed eddies (49–52° N, 167–174° E) during winter.

2.4 Model

To evaluate the temporal change in the subsurface dichothermal water of eddies, we used a re-analysis dataset (temperature, salinity, sea surface height, and geostrophic velocity) generated by a data-assimilative eddy resolving ocean model called Fisheries Research Agency Regional Ocean Model System (FRA-ROMS) (FRA, Japan 2014; http://fm.dc.affrc.go.jp/fra-roms/index.html). FRA-ROMS is a ROMS (Rutgers University and UCLA; http://www.myroms.org/index.php)-based ocean model. This model domain is 15–65° N and 115° E–150° W in the North Pacific. The horizontal resolution is 1/10° × 1/10°, which provides 20 points per most of eddy radii. The model vertically consists of 19 layers between 0 and 1000 m depth (0, 10, 20, 30, 50, 75, 100, 125, 150, 200, 250, 300, 400, 500, 700, 800, 900, and 1000 m). The model assimilates sea surface height and temperature and in situ vertical profiles of temperature and salinity in the North Pacific by three-dimensional variational method using empirical orthogonal function (EOF) joint mode (Fujii and Kamachi 2003) for subsurface hydrographic fields to match the SLA observations and then generates realistic re-analysis products. We conducted Lagrangian particle-tracking experiments at fixed depth (100, 125, and 150 m) using the FRA-ROMS velocity field to explain the changes of subsurface dichothermal water within the observed eddies. Since eddies are sometimes intensified at subsurface, we calculated correlation coefficient between the surface and the subsurface fields in the model. We calculated Okubo-Weiss parameter using FRA-ROMS flow fields at the surface and one of eddy subsurface depth (100 m). The parameter at the surface was positively correlated with that at 100 m ($R = 0.91$, $p < 0.01$). We evaluated the position of each particle by calculating an advection equation, which was inverse in time,

$$\frac{dx}{dt} = -u(x, y, t), \frac{dy}{dt} = -v(x, y, t)$$

where (x (t), y (t)) is position of a particle at time (t), and (u, v) is velocity at position (x, y) at time (t). The temporal resolution was 80 min, which is smaller than the eddy turnover time (about 3 days). By linear interpolation, (u, v) is estimated from FRA-ROMS velocity field. We initially released 1275 particles for Eddy A, 1775 particles for Eddy B, and 1475 particles for Eddy C inside the approximate area around the center of each eddy at the date of in situ observations (either July 7, 2010 or June 13, 2012) (Fig. 7). The released areas were surrounded by boundary lines of the FRA-ROMS sea surface height with −0.70 m for Eddy A, −0.60 m for Eddy B, and −0.64 m for Eddy C. We conducted a particle-backtracking experiment and examined temporal change in the locations of released particles to pursue the origin of dichothermal water and evaluated temperature changes in the eddies.

3 Results

3.1 Observed hydrographic structure of the Aleutian eddies

On the basis of SLA (Fig. 1b, c), the stations from 167.84° to 168.78° E, the stations from 171.35° to 173.49° E, and the stations from 170.99° to 172.49° E were located inside Eddies A, B, and C, respectively. Within the three mesoscale anticyclonic eddies, subsurface dichothermal water was commonly observed at a depth of 50–200 m and 26.3–26.5 σ_θ isopycnal surfaces (Fig. 2a, c, e). At the depth of dichothermal water, salinity ranged between 33.1 and 33.2 psu (Fig. 2b, d, f). Near the centers of eddies, the dichothermal water in Eddies A and C contained patches of colder temperature water (2.5–3.0 °C) at 100–150 m (Fig. 2a, e) and were relatively colder than that in Eddy B (3.0–4.0 °C) (Fig. 2c). In the eastern edge of Eddy A, a further colder dichothermal water (2.0–2.5 °C) was also observed at about 100–200 m and about 26.55σ_θ isopycnal surface between 167.78 and 169.66° E (Fig. 2a). The salinity of this colder water ranged between 33.2 and 33.3 psu (Fig. 2b). Nevertheless, this colder water was not seen within the other two eddies. Underneath the dichothermal water, a subsurface mesothermal water of 4.0–4.5 °C was observed in every eddy at depth of 200–500 m and 26.5–26.9 σ_θ isopycnal surfaces (Fig. 2a, c, e). At the depth of mesothermal water, salinity ranged between 33.4 and 33.8 psu (Fig. 2b, d, f). The mesothermal water was also warmer than the water outside of eddies in the west (3.5–4.0 °C). This water within Eddy A was warmer than the water outside the both sides of eddy (Fig. 2a).

Figure 3 shows temperature-salinity relationship at stations inside the three observed Aleutian eddies. The subsurface dichothermal water and mesothermal water were separated at density of 26.5–26.6 σ_θ. The maximum temperature in the mesothermal water was about 4.2 °C at about 26.7 σ_θ among the three eddies. Therefore, the warmer mesothermal

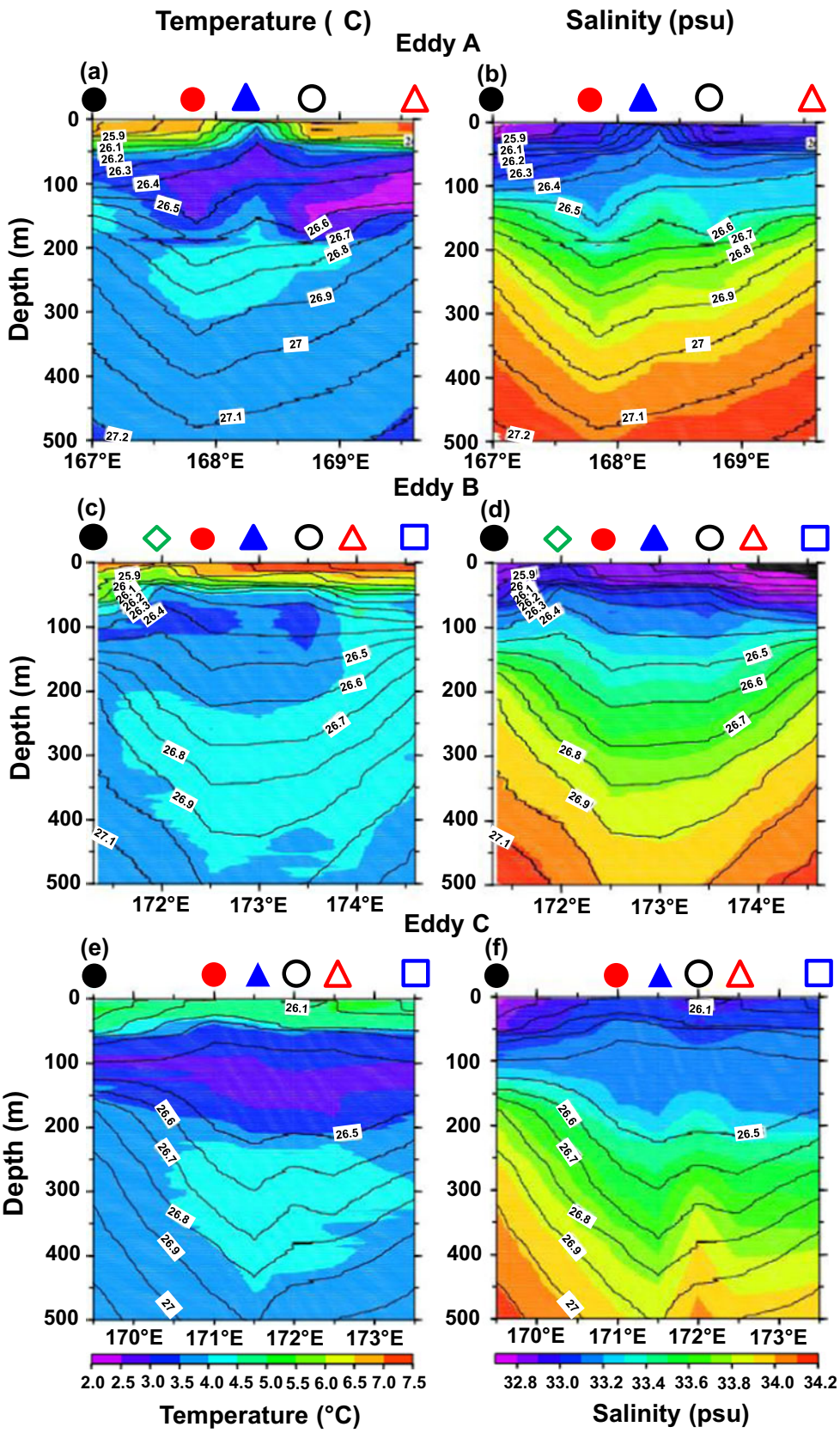

Fig. 2 Temperature (°C as color contour scale) and salinity (psu as color contour scale) distributions superimposed by density distribution (σ_θ as contour) at a depth of 0–500 m for the stations crossing Eddy A (**a**, **b**), Eddy B (**c**, **d**), and Eddy C (**e**, **f**) (the cast symbols are referred to the symbols in Fig. 1b and c)

water (4.0–4.2 °C at about 26.7–26.8 σ_θ) within these eddies is considered as a hydrographic character of Aleutian eddies.

The minimum temperature in the dichothermal water was observed commonly at about 26.4 σ_θ isopycnal surface

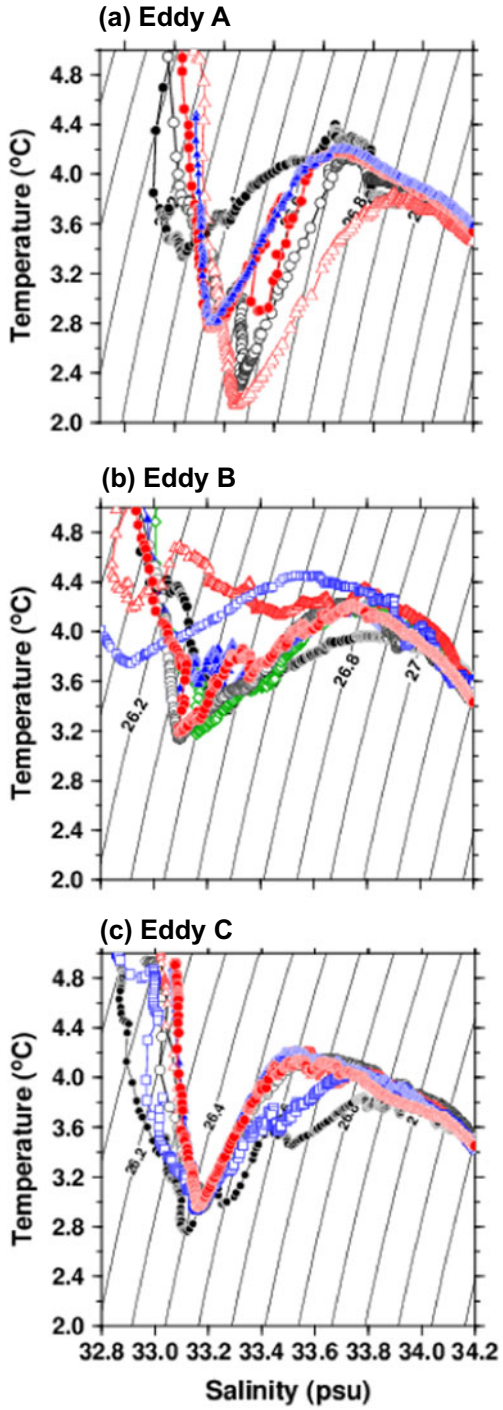

Fig. 3 Temperature and salinity (TS) relationship for the stations within Eddy A (**a**), Eddy B (**b**), and Eddy C (**c**) (reference to Figs. 1 and 2)

among the three eddies, and the minimum temperatures were relatively colder in Eddies A and C (2.8–2.9 °C) than in Eddy B (3.2 °C). The colder minimum temperatures in Eddies A and C than in Eddy B are possibly due to different physical oceanographic environments that these eddies experienced during the propagation. What happens to these eddies will be further described in the following sections.

Fig. 5 Time series of area (*solid triangles*) and sea level anomaly at the center as strength of eddy (*open squares*) of mesoscale anticyclonic eddies calculated from altimetry data in 7-day intervals for Eddy A (**a**), Eddy B (**b**), and Eddy C (**c**). Time series of mean mixed layer depth (*solid circles*) in the core areas of Eddy A (**d**), Eddy B (**e**), and Eddy C (**f**). Each *inverted triangle* indicates the date of in situ observation. Time scales are different between upper two plots (Eddies A and B) and a lower plot (Eddy C)

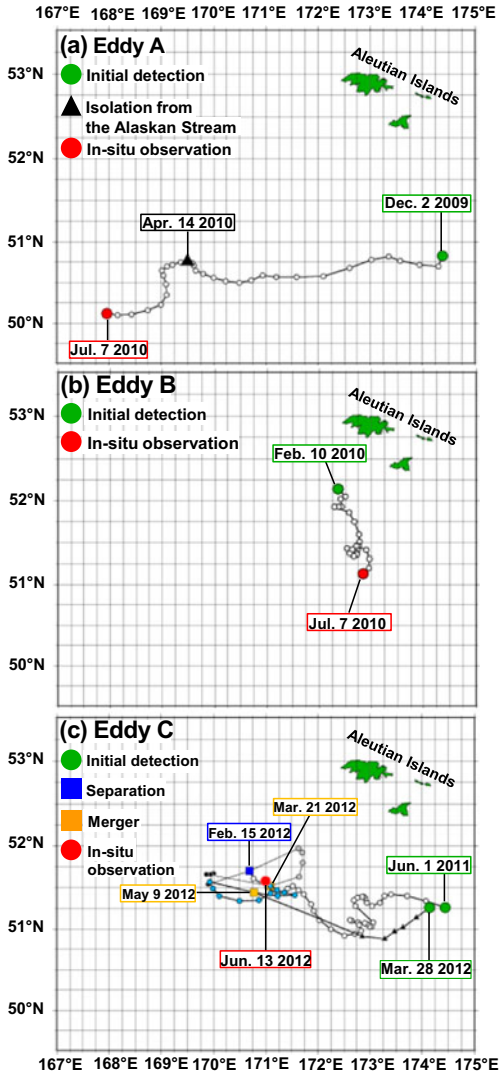

Fig. 4 History of mesoscale anticyclonic eddies for Eddy A (**a**), Eddy B (**b**), and Eddy C (**c**) in 7-day intervals. A symbol indicates the center of eddy in each period calculated from altimetry data. For Eddy C (**c**), *black* and *gray circles* show the centers of two eddies from February 15 to March 21, 2012, and *blue circles* indicate the center of eddy after March 21. The *triangle* indicates the center of eddy merging with Eddy C on May 9

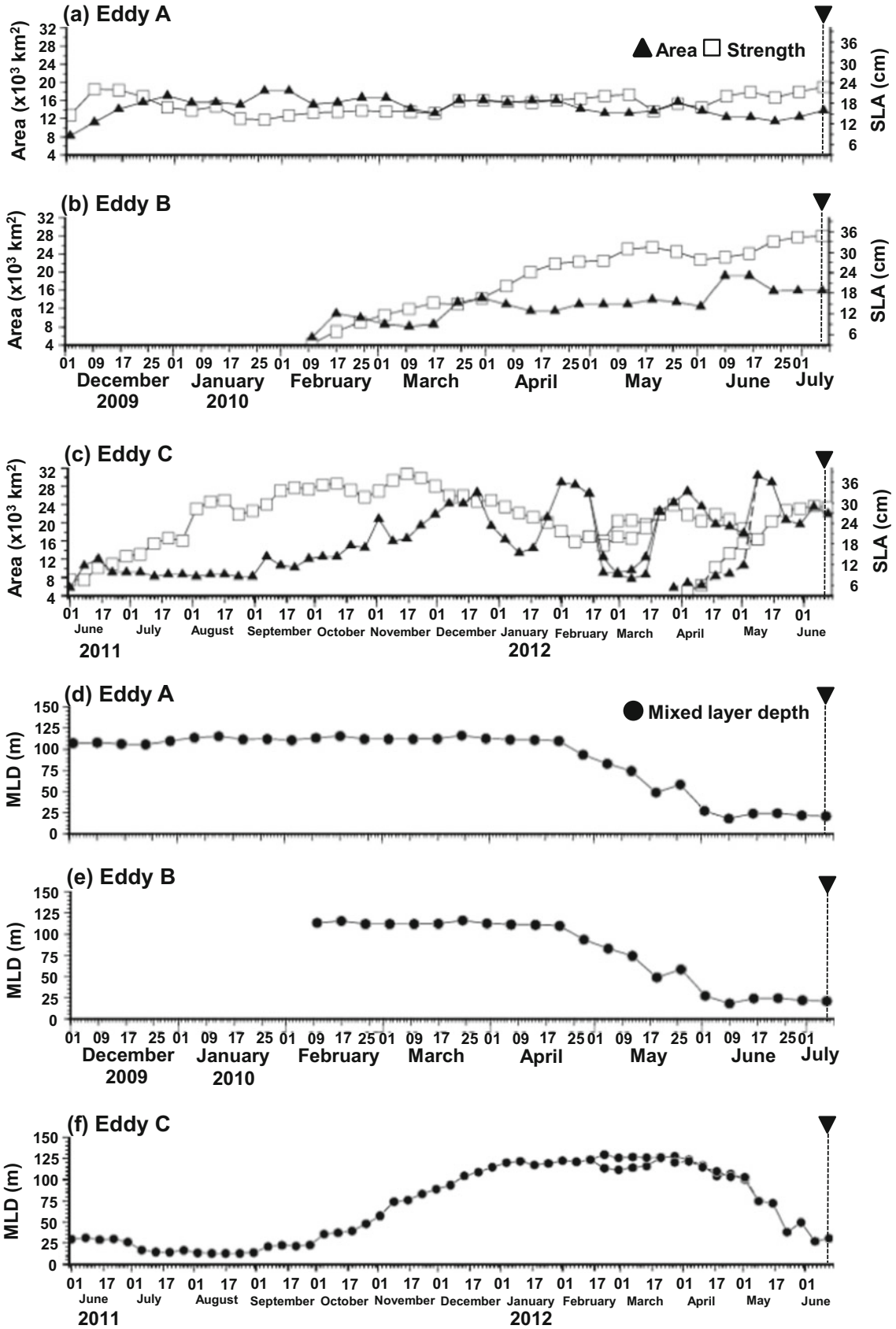
(a) Eddy A
Area (x10³ km²)
SLA (cm)
Area
Strength
(b) Eddy B
December 2009
January 2010
February
March
April
May
June
July
(c) Eddy C
June
July
August
September
October
November
December
January
February
March
April
May
June
2011
2012
(d) Eddy A
MLD (m)
Mixed layer depth
(e) Eddy B
(f) Eddy C

3.2 History of observed Aleutian eddies

Each eddy had different propagation history from its initial detection to the in situ observation. Eddy A was first detected in the early December 2009 south of the Aleutian Islands (location of the eddy center: 50° 49′ N, 174° 22′ E) and moved westward in the first 6 months (Fig. 4a). Based on an ADT data, this eddy was isolated from the Alaskan Stream in the mid-April 2010 as its outer edge (about 10–12 cm in ADT) detached from the Alaskan Stream (Electronic supplementary Fig. S1). After the isolation from the Alaskan Stream, the eddy propagated southwestward and reached the location of in situ observation (near 50° 07′ N, 167° 57′ E). The eddy area based on Okubo-Weiss parameter ($W < -2 \times 10^{-12}$ s^{-2}) increased from ~8 to ~18×10^3 km^2, and the SLA near the center, an indicator of eddy strength, also increased from ~15 to ~24 cm (Fig. 5a) in the first month of westward propagation. As this eddy continuously propagated southwestward to the site of in situ observation in the next 6 months, the area stayed between ~16 and ~20×10^3 km^2 and the strength was kept between ~18 and ~20 cm. The mean mixed layer depth (MLD) within the core area of Eddy A calculated from FRA-ROMS re-analysis dataset was deeper between the early December 2009 and the mid-April 2010 (105.8–111.5 m) than that between the late April and the in situ observation in the early July (17.9–93.5 m) (Fig. 5d).

Eddy B was initially observed south of the Aleutian Islands (location of the center: 52° 10′ N, 172° 50′ E) in the early February in 2010 (Fig. 4b). In contrast to Eddy A, this eddy propagated mostly south to southeastward and reached the site of in situ observation (around 51° 10′ N, 172° 50′ E). In contrast to Eddy A, Eddy B continuously increased its area from ~7 to ~18×10^3 km^2 (Fig. 5b) and its strength from ~6 to ~35 cm (Fig. 5e) as it moved southeastward from the initial site of detection to the site of in situ observation. This eddy was not isolated from the Alaskan Stream region. Similar to the core area of Eddy A, the MLD in Eddy B also shifted seasonally. It ranged between 109.8 and 116.2 m before the mid-April 2010 and became shallower in depth (48.9–93.5 m) during the late April and May (Fig. 5e).

Similar to Eddy A, Eddy C (open circles) was initially detected south of the Aleutian Islands (location of the center: 51° 15′ N, 174° 26′ E) in the early June 2011 and moved westward in the next 8 months (Fig. 4c). Unlike the other two eddies, this eddy separated to two distinctive eddies (the solid black and gray circles, respectively) in the mid-February 2012, and then the two merged into a single eddy in the late March. In the early May, this eddy merged with other eddy (solid black triangle) initially detected south of the Aleutian Islands (location of the center: 51°15′ N, 174° 08′ E) in the late March and reached the site of in situ observation (near 51° 34′ N, 171° 00′ E) in the early July 2012. As Eddy C propagated westward from June 1 to December 14, 2011 (Fig. 4c), the area steadily increased from ~6 to ~28×10^3 km^2 and the strength from ~6 to ~38 cm (Fig. 5c). When the eddy was separated into two eddies between February 15 and March 21, 2012 (Fig. 4c), the area rapidly decreased from ~26 to ~7×10^3 km^2 (Fig. 5c). After the two eddies merged into a single eddy on March 21, the area recovered from ~7 to ~22×10^3 km^2. During the period of the eddy separation, the strength remained around ~20 cm. After Eddy C merged with another eddy propagating westward from 51° 15′ N, 174° 08′ E, the area increased from ~18 to ~30×10^3 km^2. Similar to the other two observed eddies in 2010, MLD calculated from FRA-ROMS re-analysis products in the core area of Eddy C demonstrated a seasonal shift (Fig. 5f).

The three eddies observed during the summers of 2010 and 2012 (Eddies A, B, and C) were recognized as Aleutian eddies since they were first detected within the Alaskan Stream region between 180° meridian and 170° E, the formation region of Aleutian eddies (Rogachev et al. 2007). Difference in the eddy history potentially influenced the hydrographic structures of eddies, particularly the subsurface dichothermal water.

Fig. 6 Horizontal distribution of FRA-ROMS re-analysis temperature superimposed by the sea surface height and geostrophic velocity at a depth of 100 m on January 1 (**a**, beginning of winter), February 14 (**b**, mid-winter), March 31 (**c**, end of winter), and July 7 (**d**, in situ observation), 2010. *White contours* and *red contours* indicate approximate area near the center of Eddy A and Eddy B, respectively. FRA-ROMS temperature distribution on January 1 (**e**, beginning of winter), February 15 (**f**, mid-winter), March 31 (**g**, end of winter), and June 13 (**h**, in situ observation), 2012. *Blue contours* indicate approximate area near the center of Eddy C

3.3 Temporal changes in the subsurface dichothermal water

The three eddies experienced different temporal changes in the dichothermal waters from winter to spring. Figure 6 shows horizontal temperature distribution from FRA-ROMS re-analysis dataset at depth of 100 m, where the subsurface dichothermal water was observed within the eddies. Temperature near the approximate center of Eddy A (white boundary line) decreased from 4.2–4.4 °C in the beginning of winter to 3.1–3.3 °C in the end of winter (Fig. 6a, b, c). Even during the spring warming period, the temperature continuously decreased to 2.7–2.9 °C on July 7, when the in situ observation was operated (Fig. 6c, d). Re-analysis temperature near the approximate center of Eddy B (red boundary line) decreased from 3.8–3.9 °C in the mid-winter to 3.2–3.4 °C in the end of winter, and then, it increased to 3.6–3.8 °C on July 7 when the in situ observation was performed (Fig. 6d). Re-analysis temperature near the approximate center of Eddy C (blue boundary line) decreased from 4.1–4.2 °C in the beginning of winter to 3.2–3.3 °C in the end of winter (Fig. 6e, f, g).

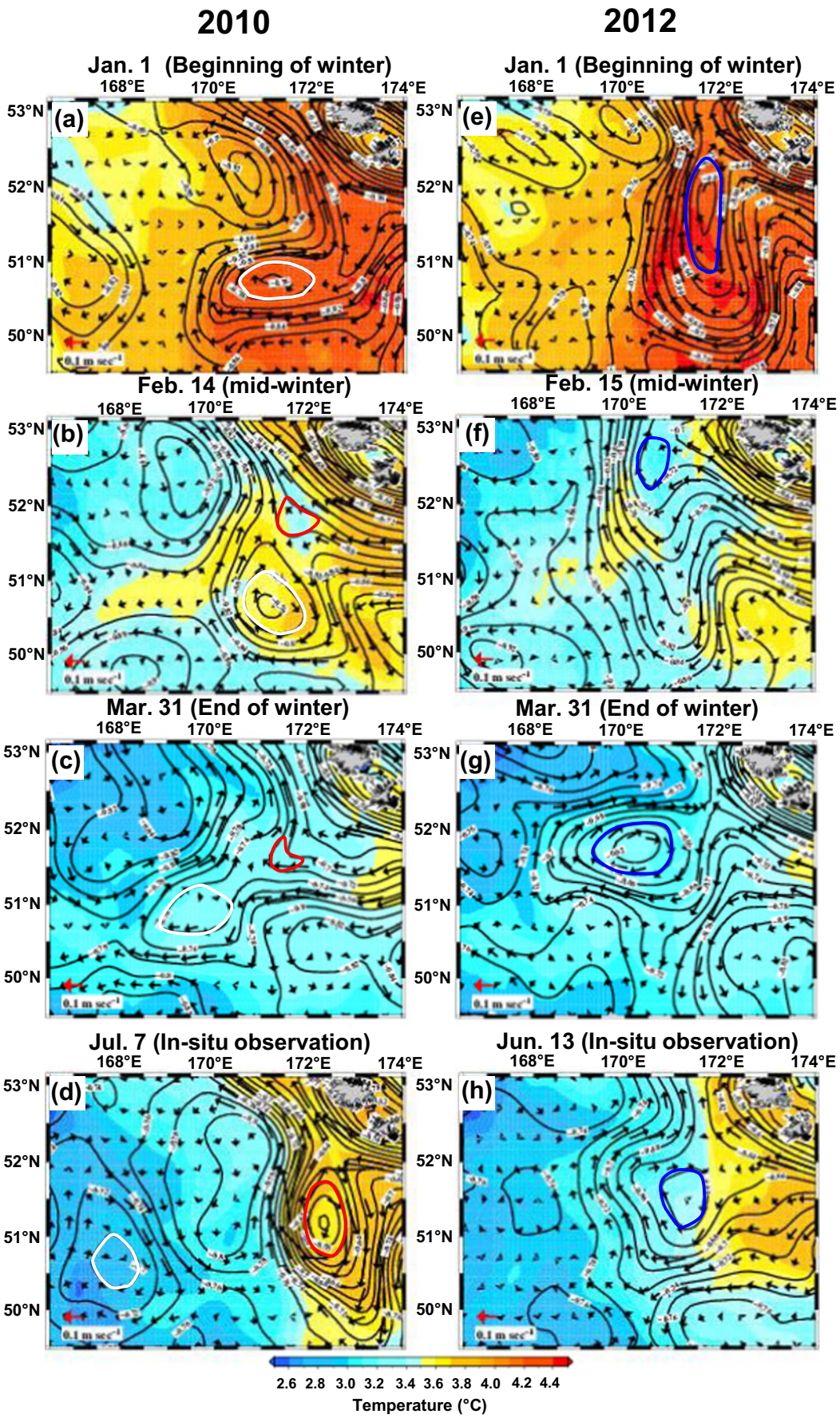
2010
2012
Jan. 1 (Beginning of winter)
Jan. 1 (Beginning of winter)
Feb. 14 (mid-winter)
Feb. 15 (mid-winter)
Mar. 31 (End of winter)
Mar. 31 (End of winter)
Jul. 7 (In-situ observation)
Jun. 13 (In-situ observation)
(a)
(b)
(c)
(d)
(e)
(f)
(g)
(h)
168°E
170°E
172°E
174°E
53°N
52°N
51°N
50°N
0.1 m sec⁻¹
2.6 2.8 3.0 3.2 3.4 3.6 3.8 4.0 4.2 4.4
Temperature (°C)

The temperature then increased to 3.4–3.6 °C by June 13, when the in situ observation was operated (Fig. 6h).

Figure 7a shows the result of particle-backtracking experiment evaluating the origin of subsurface dichothermal water

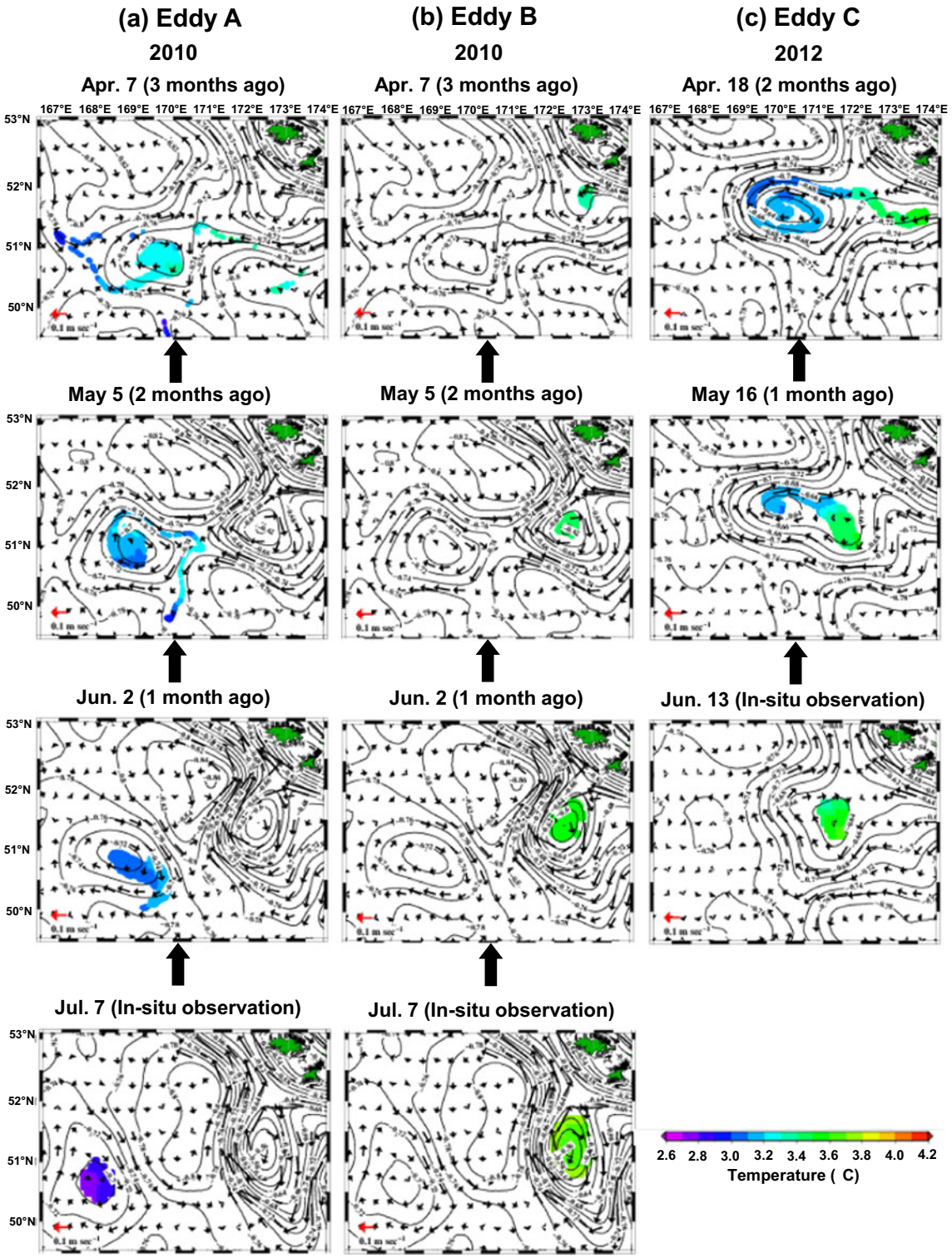

Fig. 7 Monthly results of particle-tracking experiments at a depth of 100 m in backward calculation for Eddy A (**a**), Eddy B (**b**), and Eddy C (**c**) from early summer to spring. The *particle* and the *color scale* indicate position of water and the corresponding temperature. Boundary line and vector are sea surface height and geostrophic velocity from FRA-ROMS re-analysis dataset

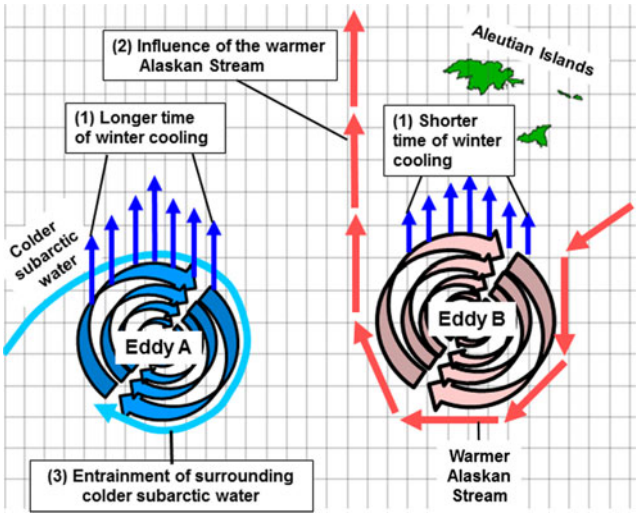

Fig. 8 A schema of major factors cooling the subsurface dichothermal water of observed Aleutian eddies

observed within Eddy A that experienced cooling even during the spring warming period. FRA-ROMS re-analysis temperature at 100 m depth within the area of Eddy A decreased from 3.2–3.3 °C in April 2010 to 3.0–3.1 °C in June 2010. The result of the experiment (Fig. 7a) suggested that in April, the area of Eddy A with cold core temperature of 3.2–3.3 °C entrained surrounding colder water of 3.0–3.1 °C. As a result, the temperature in the eddy core decreased to 3.1–3.2 °C in May.

In contrast to Eddy A, core temperature of both Eddies B and C slightly increased during spring warming period (Fig. 7b, c). Re-analysis temperature in the approximate area of Eddy B slightly increased from 3.3–3.5 °C in April to 3.6–3.8 °C in July (Fig. 7b). Re-analysis temperature in the core of Eddy C also increased from 3.4–3.5 °C in April to 3.3–3.6 °C in June (Fig. 7c). In April, Eddy C entrained surrounding water into the core, possibly originated from the Alaskan Stream. The similar patterns were observed in the results of particle-backtracking experiments at the other depth (125 and 150 m) where the subsurface dichothermal water was observed in the in situ observations (Electronic supplementary Figs. S2 and S3).

4 Discussion

The dichothermal water in the three observed Aleutian eddies was considered to be affected by the following three major factors, (1) time length of winter cooling, (2) influence of warmer Alaskan Stream, and (3) entrainment of surrounding colder subarctic water (Fig. 8). Table 1 shows a summary of the above factors on the subsurface dichothermal water of observed Aleutian eddies. Time length of winter cooling was shorter in Eddy B (about 1.5 months; February 10–March 31 2010) than in the other two eddies (at least 3 months), which were formed prior to January. Shorter winter cooling possibly resulted in smaller decrease (about −0.4 °C) in FRA-ROMS re-analysis temperature near the center of Eddy B from February to March (Fig. 6) than in the other two eddies (decrease of about −0.8 to −0.9 °C from January to March). Satellite sea surface temperature (The Group for High Resolution Sea Surface Temperature Science Team [GHRSST], PODAAC, NASA, USA 2011) also decreased from 4.0–4.5 °C in January to 2.5–3.0 °C in March 2010. This decrease in the satellite observed sea surface temperature was consistent with the temperature change in FRA-ROMS re-analysis dataset, which reflected the observed value.

Climatological net upward heat flux in the approximate areas of the observed three eddies (49–52° N, 167–174° E) between February and March (ranging from −67.9 to −104.8 W m^{-2}, mean −88.2 W m^{-2}) is smaller than that between January and March (ranging from −182.9 to −231.9 W m^{-2}, mean −211.5 W m^{-2}). Decrease in temperature at depth of 0–100 m from February to March estimated from the net heat flux between February and March (ranging between −0.35 and −0.23 °C, mean −0.29 °C) is smaller than that from January to March (ranging between −1.19 and −0.94 °C, mean −1.09 °C). During winter, the MLD in the core area of Eddy A was below 100 m depth (Fig. 5e) and could enhance the cooling of dichothermal water as well as the net heat flux from ocean to atmosphere. FRA-ROMS vertical temperature was 4.10 ± 0.32 °C along transect crossing Eddy A in dichothermal layer (depth of 100–150 m) in early December (Fig. 9a). The vertical temperature became relatively uniform in the upper 100-m water column in January and decreased from 3.78 ± 0.24 °C in January to 2.99 ± 0.19 °C in March (Fig. 9b, c, d). This result suggests strong winter atmospheric cooling on this

Table 1 A summary of major factors affecting formation of subsurface dichothermal water in the observed Aleutian eddies

Eddy	1. Time length of winter cooling (month)	2. Influence of Alaskan Stream	3. Entrainment of colder water (month)
A	~3	Until April 2010	~2
B	~1.5	○	N/A
C	~3	○	N/A

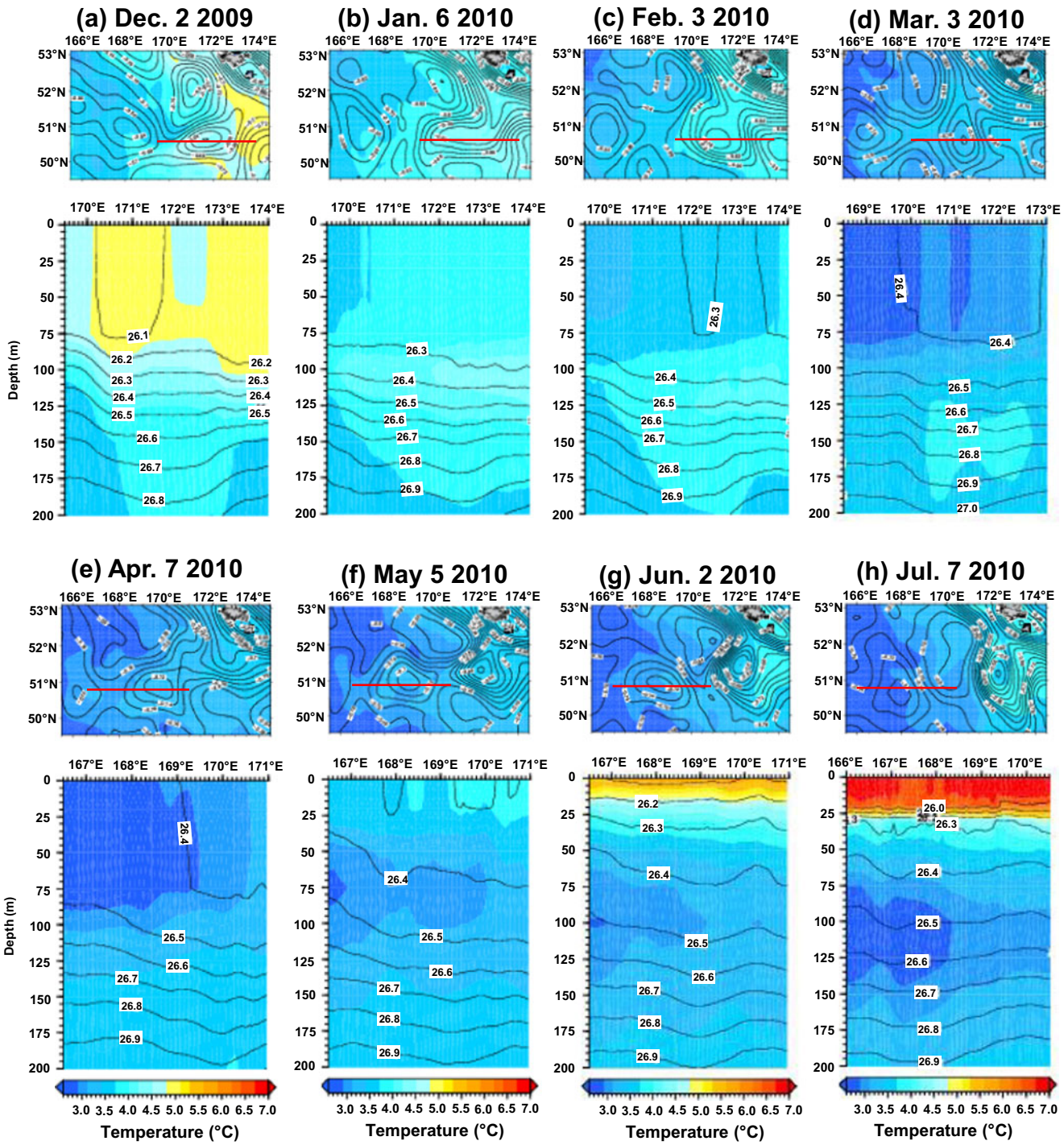

Fig. 9 Temporal change in vertical FRA-ROMS temperature distribution (°C in color) superimposed by density distribution (σ_θ, contour) at a depth of 0–200 m in transects crossing Eddy A from January to July 2010. For each month, an *upper panel* shows horizontal temperature distribution, and the *lower panel* indicates vertical FRA-ROMS temperature and density distributions

layer, decreasing the dichothermal temperature during winter although Eddy A was within the Alaskan Stream region (Fig. 4a, Electronic supplementary Fig. S1).

From April to June, sea surface temperature (GHRSST) in the studied area increased from 2.5–3.0 °C to 4.5–5.5 °C; thus,

Fig. 10 The results of particle-tracking experiment in backward ▶ calculation in a 7-day interval for Eddy A at depth of 100 m during April through May 2010. *Boundary lines* and *vectors* are sea surface height and geostrophic velocity from FRA-ROMS re-analysis dataset

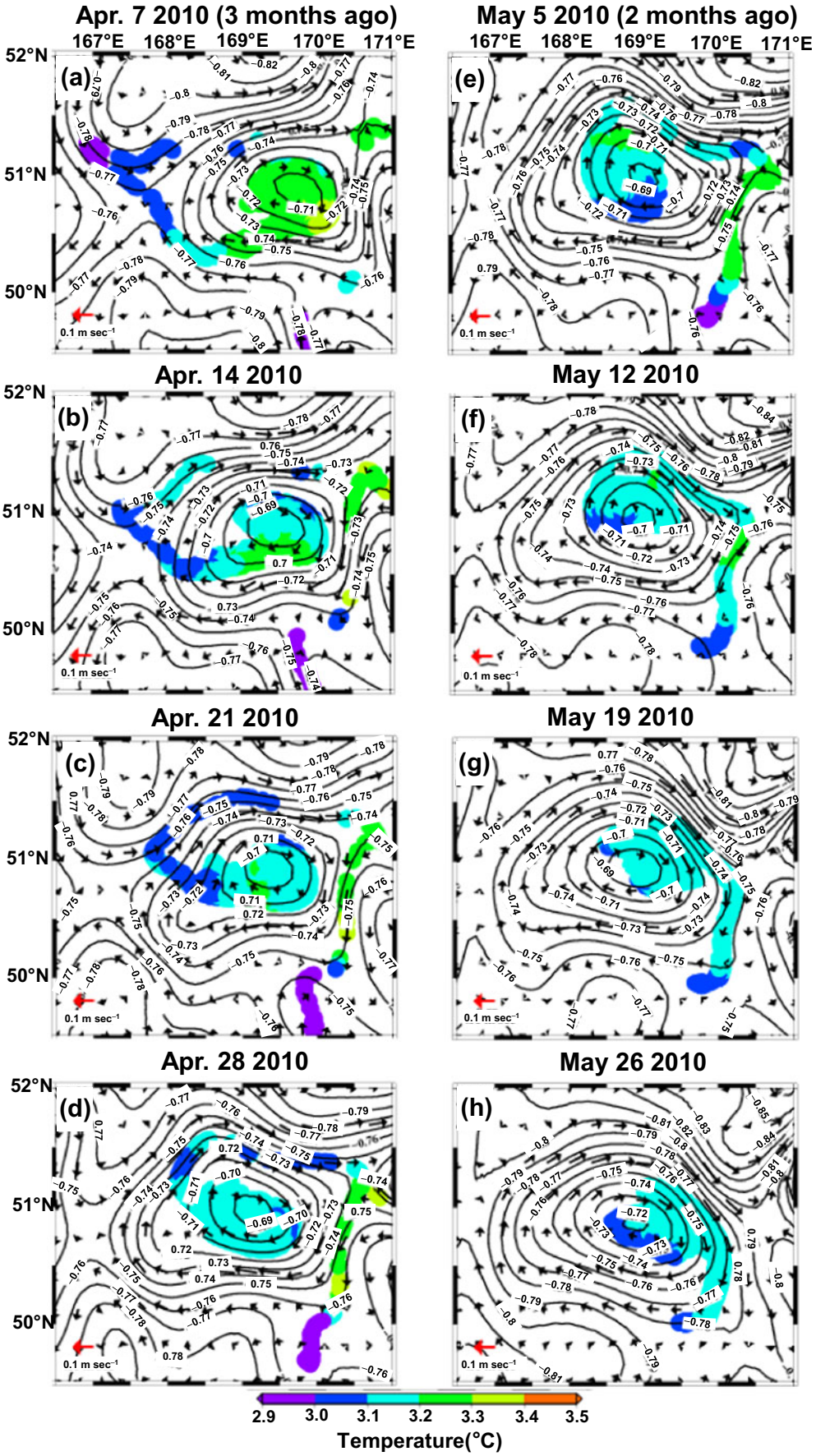
Apr. 7 2010 (3 months ago)
May 5 2010 (2 months ago)
Apr. 14 2010
May 12 2010
Apr. 21 2010
May 19 2010
Apr. 28 2010
May 26 2010
(a)
(b)
(c)
(d)
(e)
(f)
(g)
(h)
167°E
168°E
169°E
170°E
171°E
52°N
51°N
50°N
0.1 m sec⁻¹
2.9
3.0
3.1
3.2
3.3
3.4
3.5
Temperature(°C)

this period was considered as spring warming period. FRA-ROMS surface temperature in the upper 20-m depth along transect crossing Eddy A also increased from 2.91 ± 0.06 °C in April to 5.10 ± 0.58 °C in June (Fig. 9e, f, g). During this warming period, the climatological net heat flux from atmosphere to sea surface (downward heat flux) in the approximate area of observed eddies is 304.4–338.2 W m^{-2} (mean 321.2 W m^{-2}), and the estimated

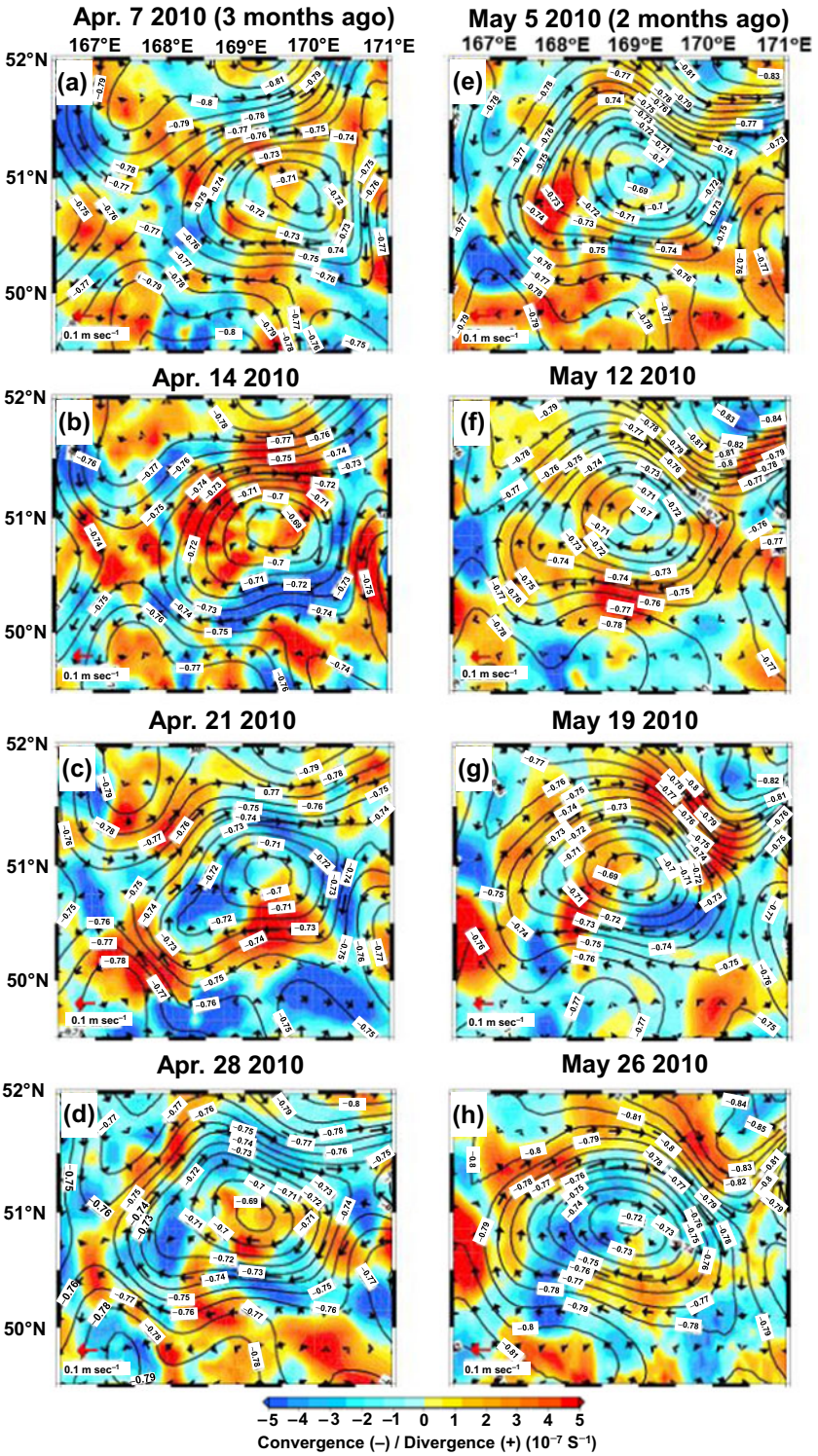

Fig. 11 The convergence and divergence around the area of Eddy A at a depth of 100 m during April through May 2010. *Boundary lines* and *vectors* are sea surface height and geostrophic velocity from FRA-ROMS re-analysis dataset

temperature increase at depth of 0–100 m was 1.58–1.76 °C (mean 1.67 °C). During the spring warming period, Eddy A was detached from the Alaskan Stream region and propagated southwestward (Fig. 4a, Table 1, Electronic supplementary Fig. S1), whereas Eddies B and C stayed within the Alaskan Stream region. The detachment from the Alaskan Stream region could make a difference in temperature distribution in the subsurface dichothermal water during the spring. Satellite sea surface temperature in the approximate area of Eddy A increased from 2.5–3.0 °C in April to 4.5–5.0 °C in June (+2.0 °C), whereas the temperature in Eddy B increased from 2.5–3.0 °C in April to 5.0–5.5 °C in June (+2.5 °C). In addition, the warmer Alaskan Stream presumably affected the surface and subsurface temperatures of Eddy B. In the previous studies (Ueno et al. 2010; Stabeno and Hristova 2014), mesoscale anticyclonic eddies in the Alaskan Stream have been observed to force the flow path of the warmer Alaskan Stream offshore and caused southward advections and meanders. In the present study, the southward meander was detected around Eddy B during the spring (Fig. 7b). The warmer Alaskan Stream potentially influenced Eddy B and increased the temperature in its dichothermal water.

After the isolation from the Alaskan Stream, Eddy A presumably entrained surrounding colder subsurface dichothermal water as it propagated southwestward from April to May 2010. Based on the climatological net surface heat flux, the temperature at 0–100 m water column was suggested to increase during the spring warming period. However, the temperature of dichothermal water near the center of Eddy A continuously decreased from 3.1–3.3 °C in the end of winter to 2.7–2.9 °C in the early July, when in situ observation was operated (Fig. 6c, d). In the in situ observation, a colder subsurface dichothermal water (2.0–2.5 °C) was found at depth of 100–150 m on the eastern side of Eddy A (Fig. 2a). This colder water was thought to recently enter the eddy from the east and spend a shorter time within it than the water in the west. FRA-ROMS vertical temperature in dichothermal layer (depth of 100–150 m) along transect crossing Eddy A decreased from 3.39 ± 0.19 °C in April to 3.18 ± 0.11 °C in June (Fig. 9e, f, g). The vertical temperature continuously decreased to 2.87 ± 0.12 °C in July, suggesting that colder dichothermal water from the west entered Eddy A between June and July (Fig. 9g, h).

Figure 10 shows the results of a particle-backtracking experiment of Eddy A at 100 m depth in a 7-day interval from April 7 to May 26, 2010. As Eddy A rotated clockwise at geostrophic velocity of 0.035–0.067 m s^{-1} at a depth of 100 m, the eddy was suggested to slowly entrain surrounding colder water from the early April to the late May. Additionally, convergence (-1.28×10^{-9} to -1.73×10^{-7} s^{-1}) calculated from FRA-ROMS re-analysis horizontal velocity field at a depth of 100 m covered a larger region than divergence (1.40×10^{-8}–8.87×10^{-8} s^{-1}) during the spring (Fig. 11). Thus, the entrainment of surrounding colder subarctic water into the core of Eddy A is presumably one of the factors decreasing the temperature of dichothermal water during the spring warming period.

In contrast to the dichothermal water showing the distinctive features and modifications among the observed eddies, mesothermal water at depth of 200–500 m demonstrated similarity among the three eddies (Fig. 2). In the in situ observation, Eddy A, isolated from the influence of Alaskan Stream, included the mesothermal water (4.0–4.5 °C), which was warmer than the outside of eddy (3.5–4.0 °C) at depth of 200–300 m (Fig. 2a). These results indicated that the subsurface dichothermal water presumably changes over time with heat exchange with atmosphere during winter and the influence of surrounding colder water during spring, whereas the mesothermal water underneath the dichothermal water possibly keeps the original feature from the Alaskan Stream region to the Western Subarctic Gyre as an Aleutian eddy propagates westward.

Furthermore, mesoscale cyclonic eddies were observed between Eddy A and Eddy B in 2010 and west of Eddy C in 2012 (Fig. 1b, c). Eddy-eddy interaction between the two eddies could have occurred (Ueno et al. 2012), which was not observed in the numerical experiments (Fig. 7a and Electronic supplementary Figs. S2 and S3). This interaction potentially resulted in an increase in eddy area, and horizontal mixing between the water inside an eddy and the water outside. It is uncertain whether other mesoscale cyclonic eddies influenced the observed eddies. In the future, long-term field analyses of Aleutian eddies are required to understand formation and modification of subsurface core waters in the eddies along with numerical simulations using re-analysis dataset from a vertically higher-resolution ocean model.

5 Conclusions

Temporal changes of the subsurface hydrographic structure in the three Aleutian eddies were studied by using ship observations, satellite observations, and re-analysis data. The subsurface temperature maxima (mesothermal water) were common among the three eddies and maintained their Alaskan Stream characteristics, whereas the subsurface temperature minimum (dichothermal water) has a wider variety depending on the time length of winter cooling, the entrainment of surrounding colder water, and the influence from the warmer Alaskan Stream. The Aleutian eddy (Eddy A) observed in the west of 170° E isolated from the Alaskan Stream contained colder subsurface dichothermal water than the other two eddies east of 170° E (Eddies B and C). This colder dichothermal water is suggested to be caused by the relatively longer winter cooling

and the subsequent cooling due to the entrainment of surrounding colder subarctic water west of 170° E even during spring warming period. The warmer dichothermal water of the eddy east of 170° E (Eddies B and C) that stayed closed to the Alaskan Stream region maintained the original core water from the late winter and were possibly influenced by warmer Alaskan Stream during spring atmospheric warming.

Acknowledgments We express our thanks to the captain, officers, and crew members of T/S Oshoro-maru, School of Fisheries Sciences, Hokkaido University and the members of Physical Oceanography Laboratory, Graduate School of Fisheries Sciences, Hokkaido University for their help in data collection at sea. The altimeter products were produced by SSALTO/DUCSCS and distributed by AVISO with support from Collecte Localisation Satellites. The FRA-ROMS re-analysis dataset were generated and provided by National Research Institute of Fisheries Science, Fisheries Research Agency of Japan. The sea surface temperature (GHRSST) was provided by Physical Oceanography Distributed Active Archive Center, NASA Jet Propulsion Laboratory. The climatological net surface heat flux was produced and provided by National Oceanography Centre, Natural Environment Research Council. The present study was partially supported by Grant-in-Aid for JSPS Fellows 25–271, KAKENHI Grant 25257206/15H05818 of the Japan Society for the Promotion of Science (JSPS). We also thank Professor Joerg-Olaf Wolff, Chief Editor; Dr. Pierre De Mey, Associate Editor of Ocean Dynamics; and two anonymous reviewers. Their valuable comments were helpful and greatly improved the present manuscript.

References

Brown MT, Lippiatt SM, Lohan MC, Bruland KW (2012) Trace metal distributions within a Sitka eddy in the northern Gulf of Alaska. Limnol Oceanogr 57(2):503–518. doi:10.4319/lo.2012.57.2.0503

Chelton DB, Schlax MG, Samelson RM, de Szoeke RA (2007) Global observations of large oceanic eddies. Geophys Res Lett 34, L15606. doi:10.1029/2007GL030812

Collecte Localisation Satellites (2014) SSALTO/DUACS user handbook: (M) SLA and (M) ADT near real time and delayed time products, version 4 rev. 1, rep. SALP-MU-P-EA-21065-CLS. CLS, Ramonville-St-Agne, France, p 72

Crawford WR (2005) Heat and fresh water transport by eddies into the Gulf of Alaska. Deep-Sea Res II 52:893–908. doi:10.1016/j.dsr2.2005.02.003

Crawford WR, Brickley PJ, Thomas AC (2007) Mesoscale eddies dominate surface phytoplankton in northern Gulf of Alaska. Prog Oceanogr 75:287–303. doi:10.1016/j.pocean.2007.08.016

Favorite F (1967) The Alaskan Stream. In N Pac Fish Comm Bull 21:1–20, http://www.npafc.org/new/inpfc/INPFC%20Bulletin/Bull%20No.21/Bull21%20p1-20%20%28Favorite%29.pdf

Fujii Y, Kamachi M (2003) A reconstruction of observed profiles in the sea east of Japan using vertical coupled temperature-salinity EOF modes. J Oceanogr 59(2):173–186. doi:10.1023/A:1025539104750

GHRSST Science Team (2011) The recommended GHRSST data specification (GDS) 2.0, document revision 4. The GHRSST International Project Office, Physical Oceanography Distributed Active Archive Center, NASA Jet Propulsion Laboratory, DAAC, Pasadena, p 123

Grist JP, Josey SA (2003) Inverse analysis adjustment of the SOC air-sea flux climatology using ocean heat transport constraints. J Clim 16(20):3274–3294. doi:10.1175/1520-0442(2003)016<3274:IAAOTS>2.0.CO;2

Henson SA, Thomas AC (2008) A census of oceanic anticyclonic eddies in the Gulf of Alaska. Deep-Sea Res I 55:163–176. doi:10.1016/j.dsr.2007.11.005

Hokkaido University (2011) Data record of oceanographic observation and exploratory fishing no. 54. In: Saitoh, SI (ed) Faculty of Fisheries Sciences, Hokkaido University, Hakodate, Japan, p 192

Ikenoue T, Ueno H, Takahashi K (2012) *Rhizoplegma boreale* (Radiolaria): a tracer for mesoscale eddies from coastal areas. J Geophys Res 117, C04001. doi:10.1029/2011JC007728

Inatsu M (2009) The neighbor enclosed area tracking algorithm for extratropical wintertime cyclones. Atmos Sci Lett 10:267–272. doi:10.1002/asl.238

Ladd C, Kachel NB, Mordy CW, Stabeno PJ (2005) Observations from a Yakutat eddy in the northern Gulf of Alaska. J Geophys Res 110, C03003. doi:10.1029/2004JC002710

Ladd C, Mordy CW, Kachel NB, Stabeno PJ (2007) Northern Gulf of Alaska eddies and associated anomalies. Deep-Sea Res I 54:487–509. doi:10.1016/j.dsr.2007.01.006

Ohtani K (1973) Oceanographic structures in the Bering Sea. Fac Fish Hokkaido Univ 21(1):65–106, http://hdl.handle.net/2115/21855

Ohtani K, Onishi H, Kobayashi N, Anma G (1997) Baroclinic flow referred to the 3000 m reference level across the 180° transect in the subarctic North Pacific. Bull Fac Fish Hokkaido Univ 48(3):53–64, http://hdl.handle.net/2115/24162

Okubo A (1970) Horizontal dispersion of floatable particles in the vicinity of velocity singularity such as convergences. Deep-Sea Res 17(3):445–454. doi:10.1016/0011-7471(70)90059-8

Onishi H (2001) Spatial and temporal variability in a vertical section across the Alaskan Stream and Subarctic Current. J Oceanogr 57(1):79–91. doi:10.1023/A:1011178821299

Onishi H, Ohtani K (1999) On seasonal and year-to-year variation in flow of the Alaskan Stream in the central North Pacific. J Oceanogr 55(5):597–608. doi:10.1023/A:1007840802296

Prants SV, Andreev AG, Budyansky MV, Uleysky MY (2013) Impact of mesoscale eddies on surface flow between the Pacific Ocean and the Bering Sea across the Near Strait. Ocean Model 72:143–152. doi:10.1016/j.ocemod.2013.09.003

Reed RK, Stabeno PJ (1993) The recent return of the Alaskan Stream to Near Strait. J Mar Res 51(3):515–527. doi:10.1357/0022240933224025

Reed RK, Stabeno PJ (1999) Recent full-depth survey of the Alaskan Stream. J Oceanogr 55(1):79–85. doi:10.1023/A:1007813206897

Rogachev KA, Shlyk NV (2009) The increased radius of the Aleutian eddies and their long-term evolution. Russ Meteorol Hydrol 35(3):206–210. doi:10.3103/S1068373910030076

Rogachev K, Shlyk N, Carmack E (2007) The shedding of mesoscale eddies from the Alaskan Stream and westward transport of warm water. Deep-Sea Res II 54:2643–2656. doi:10.1016/j.dsr2.2007.08.017

Saito R, Yamaguchi A, Yasuda I, Ueno H, Ishiyama H, Onishi H, Imai I (2014) Influences of mesoscale anticyclonic eddies on zooplankton community south of the western Aleutian Islands during the summer of 2010. J Plankton Res 36(1):117–128. doi:10.1093/plankt/fbt087

Stabeno PJ, Hristova HS (2014) Observations of the Alaskan Stream near the Samalga Pass and its connection to the Bering Sea: 2001–2004. Deep-Sea Res I 88:30–46. doi:10.1016/j.dsr.2014.03.002

Ueno H, Yasuda I (2000) Distribution and formation of the mesothermal structure (temperature inversions) in the North Pacific subarctic region. J Geophys Res 105(C7):16885–16897. doi:10.1029/200JC900020

Ueno H, Yasuda I (2005) Temperature inversions in the subarctic Pacific. J Phys Oceanogr 35:2444–2456. doi:10.1175/JPO2829.1

Ueno H, Oka E, Suga T, Onishi H (2005) Seasonal and interannual variability of temperature inversions in the subarctic North Pacific. Geophys Res Lett 32, L20603. doi:10.1029/2005GL023948

Ueno H, Oka E, Suga T, Onishi H, Roemmich D (2007) Formation and variation of temperature inversions in the eastern subarctic North Pacific. Geophys Res Lett 34, L05603. doi:10.1029/2006GL028715

Ueno H, Freeland H, Crawford WR, Onishi H, Oka E, Sato K, Suga T (2009) Anticyclonic eddies in the Alaskan Stream. J Phys Oceanogr 39:934–951. doi:10.1175/2008JPO3948.1

Ueno H, Crawford WR, Onishi H (2010) Impact of Alaskan Stream eddies on chlorophyll distribution in the North Pacific. J Oceanogr 66(3):319–328. doi:10.1007/s10872-010-0028-6

Ueno H, Yasuda I, Itoh S, Onishi H, Hiroe Y, Suga T, Oka E (2012) Modification of a Kenai eddy along the Alaskan stream. J Geophys Res 117, C08032. doi:10.1029/2011JC007506

Weiss J (1991) The dynamics of enstrophy transfer in two dimensional hydrodynamics. Phys D 48(2–3):273–294. doi:10.1016/0167-2789(91)90088-Q